Hindawi Publishing Corporation
International Journal of Photoenergy
Volume 2014, Article ID 953623, 8 pages
http://dx.doi.org/10.1155/2014/953623

Research Article

Near Infrared Radiation as a Rapid Heating Technique for TiO_2 Films on Glass Mounted Dye-Sensitized Solar Cells

Katherine Hooper, Matthew Carnie, Cecile Charbonneau, and Trystan Watson

SPECIFIC, Baglan Bay Innovation and Knowledge Centre, College of Engineering, Swansea University, Central Avenue, Baglan SA12 7AX, UK

Correspondence should be addressed to Trystan Watson; t.m.watson@swansea.ac.uk

Received 16 July 2014; Accepted 21 September 2014; Published 6 November 2014

Academic Editor: Meenakshisundaram Swaminathan

Near infrared radiation (NIR) has been used to enable the sintering of TiO_2 films on fluorine-doped tin oxide (FTO) glass in 12.5 s. The 9 μm thick TiO_2 films were constructed into working electrodes for dye-sensitized solar cells (DSCs) achieving similar photovoltaic performance to TiO_2 films prepared by heating for 30 min in a convection oven. The ability of the FTO glass to heat upon 12.5 s exposure of NIR radiation was measured using an IR camera and demonstrated a peak temperature of 680°C; glass without the 600 nm FTO layer reached 350°C under identical conditions. In a typical DSC heating step, a TiO_2 based paste is heated until the polymeric binder is removed leaving a mesoporous film. The weight loss associated with this step, as measured using thermogravimetric analysis, has been used to assess the efficacy of the FTO glass to heat sufficiently. Heat induced interparticle connectivity in the TiO_2 film has also been assessed using optoelectronic transient measurements that can identify electron lifetime through the TiO_2 film. An NIR treated device produced in 12.5 seconds shows comparable binder removal, electron lifetime, and efficiency to a device manufactured over 30 minutes in a conventional oven.

1. Introduction

There has been extensive research into emerging solar cell technologies such as organic photovoltaics, organohalide perovskites, and dye-sensitized solar cells (DSCs) due to their potentially low production costs compared to traditional silicon [1]. DSCs have now exceeded 12% efficiency with a combination of Co(II/III) tris(bipyridyl) based electrolyte and zinc porphyrin based D-π-A dyes [2]. This increases the potential that DSCs could compete against more established thin film solar cells in the near future particularly given their transparency and potential application in glazing. However, challenges still exist in the industrial scale manufacture such as fabrication time and process bottlenecks [3].

Production time is a major barrier for translating technology from laboratory to industrial scale. In the case of DSCs, there are two long heating steps: heat treatment of a TiO_2 slurry for the working electrode at 450°C and thermal decomposition of a platinum precursor for the counter electrode at 385°C, both these heating steps require 30 min complete in a conventional oven.

The purpose of the TiO_2 heat treatment is to create a high surface area mesoporous film structure such that dye adsorption is maximised and electrolyte penetration is facilitated. Most commonly, TiO_2 nanoparticles are incorporated into a slurry or paste and deposited by doctor blading or screen printing. The nanoparticles require a means of separation to prevent aggregation and this is achieved via steric and electrostatic stabilisation. The former is a more common method and is achieved via the addition of an organic binder such as ethyl cellulose or polyethylene glycol to a TiO_2 solvent mix. This helps to prevent particles from colliding in addition to binding the colloid together for easy deposition.

To obtain a mesoporous layer from the nanoparticle containing TiO_2 paste, a heating step is required which performs two functions: (1) to remove the binder and (2) to sinter the TiO_2 particles together. The TiO_2 particles require good interconnectivity for subsequent electron diffusion to the transparent conducting oxide (TCO) layer. The typical temperature for sintering of TiO_2 is 450–500°C over a period of 30 minutes.

Alternative heating processes that have been proposed to reduce these times below 5 min include compression [4–6], microwave [7], laser [8–13], and pulsed white light sintering [14] of TiO_2 films. Using electromagnetic radiation in the near infrared (NIR) region, TiO_2 films for DSCs have been sintered onto titanium substrates in 12.5 s [15] with identical electron transport and lifetime properties [16] to conventionally heated films. This technique involves absorption of NIR radiation by the metal substrate causing a substantial rise in temperature which directionally heats the adhered coating resulting in an extremely rapid removal of binder and sintering of TiO_2 paste.

NIR heating has also been used to significantly reduce the processing time of silver inks for printed contacts [17] and the platinisation of counter electrodes for DSCs on fluorine-doped tin oxide (FTO) glass [18]. Previous work on NIR heating has involved the absorption of NIR radiation by a metallic material; however, the use of a thin 600 nm layer of FTO to process TiO_2 has never been demonstrated. This is especially relevant to DSCs where the vast majority of cells are made on FTO glass and do not suffer the reduction in efficiency typically observed on a metallic substrate [19]. This paper elaborates on the suitability of NIR heating for FTO glass mounted dye-sensitized solar cells and quantifies the temperatures profiles possible with 12.5 s exposure. Thermogravimetric analysis (TGA) has been used to measure the level of solvent and binder remaining in the TiO_2 films after exposure to NIR to determine if complete removal could be achieved in 12.5 s. DSCs were constructed from TiO_2 films heated on FTO glass and the electron transport and recombination lifetime were characterised using optoelectronic transient measurements to assess the degree of NIR induced TiO_2 sinter and interparticle connectivity.

2. Experimental

2.1. Calculating Temperature for NIR Exposed FTO Glass. The NIR equipment (NIR/IR Coil lab LV2, AdPhos) consists of a set of tungsten halogen emitters that output in the region of 250–2500 nm, peaking at between 800 and 1200 nm. The intensity of the lamps is controlled by the user as a percentage from 0 to 100 to vary the energy density of radiation. At maximum lamp power, this is 25 kW. Samples are placed on a platform that runs on a conveyor belt at a selected line speed which determines the exposure time; 2 m min^{-1} was used for this work corresponding to a 12.5 s residence time. An IR camera (thermoIMAGER TIM200, Micro-Epsilon) was used to estimate the temperature reached by the glass substrates after NIR exposure; a contact method using a thermocouple was not possible. Firstly, the emissivity of 7 Ω/□ FTO glass (NSG Pilkington) and uncoated glass of equal thickness was calculated by imaging these substrates at a known temperature on a hot plate. Using these values, FTO glass and uncoated glass were then filmed following exposure to NIR. Due to the sample platform being partially enclosed by reflectors, the samples could not be filmed during heating. Consequently, the IR camera filmed the samples as they exited the NIR emitters at their peak temperature.

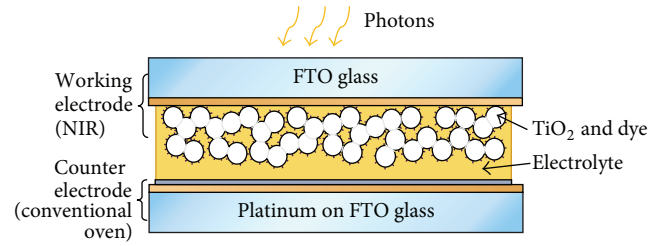

Figure 1: Schematic of the DSC architecture (electrode heating method is shown in brackets).

2.2. Preparation of NIR Heated TiO_2 Films. TiO_2 paste (DSL 18NR-AO, Dyesol) was doctor-bladed onto FTO glass and heated using 12.5 s of NIR radiation at varying lamp intensities resulting in a dry film thickness of 9 μm. TiO_2 films that had undergone the heating treatment were removed from the FTO glass and placed in a platinum crucible and their subsequent weight loss between 30 and 600°C was measured using a thermogravimetric analyser (Pyris 1 TGA, Perkin Elmer) with a ramping rate of 20°C/min in a nitrogen atmosphere. Weight loss from TGA was indicative of the level of binder removal of the TiO_2 films after NIR treatment. An effective heat treatment would mean very little binder being left over in the film; a conventional oven-treated sample was used as a comparison (450°C degrees for 30 minutes). Scanning electron microscope (SEM) images were obtained of the TiO_2 films using a FEG-SEM (S-4800, Hitachi) with beam parameters of 10–12 eV and 10 μA and a 4–12 mm working distance.

2.3. Device Fabrication and Characterisation. DSCs were fabricated using FTO glass working electrodes of 25 × 15 mm and doctor-bladed TiO_2 paste heated with 12.5 s of NIR radiation at lamp intensities between 60 and 100%. The TiO_2 films had a film thickness of 9 μm and were sensitized using 0.3 mM dye solution of N719 (Solaronix) in ethanol for 16 hours. FTO glass counter electrodes of equal dimensions were prepared by thermal platinisation of 5 mM hexachloroplatinic acid in 2-propanol at 385°C for 30 min. A schematic representation of the test device architecture can be seen in Figure 1.

Conventional (control) working electrodes were cast and dyed in a similar manner but were then heated in a convection oven at 450°C for 30 min. The working and counter electrodes were sealed together in a hot press at 120°C for 30 s using 25 μm Surlyn (Solaronix) gaskets. An electrolyte solution of 0.8 M 1-propyl-3-methylimidazolium iodide (PMII), 0.3 M benzimidazole, 0.1 M I_2, and 0.05 M guanidinium thiocyanate dissolved in 3-methoxypropionitrile was vacuum-injected into the cell through a 0.5 mm hole in the counter electrode and then sealed using Surlyn and a circular microscope coverslip. Conductive silver paint (Electrolube, Farnell) was used to create contacts on the electrodes and the devices had an active area of 1 cm^2.

The photovoltaic performance of the assembled DSCs was measured using an Oriel Sol3A solar simulator (94023A) illuminated at 1 sun (1000 W/m^2, AM1.5) calibrated using a certified monocrystalline silicon reference cell (91150V

Oriel). Transient photovoltage and photocurrent measurements, as described in [20], were made at open circuit and short circuit, respectively, to obtain the exponential decay. The bias light was provided by a custom made bank of white LEDs.

3. Results and Discussion

3.1. Absorption of NIR by FTO. FTO glass is a commonly used substrate for solar cells such as DSCs. It has the high temperature stability necessary for processing DSCs, is the least expensive TCO [21], and is deposited with high throughput during glass manufacture using atmospheric pressure chemical vapour deposition (APCVD). FTO is a heavily doped wide band gap degenerative *n*-type semiconductor which has a large concentration of free electrons. FTO is opaque in the UV region because UV photons have energy higher than its optical band gap causing interband absorption. In the visible region, where the photon energy is less than its optical band gap, there is a low probability of absorption; so, it still appears transparent when coated onto glass. However, in the infrared region, absorption by free carriers occurs. For most TCO materials (including FTO), the plasma frequency, the wavelength at which the material changes from a metallic to a dielectric response, falls in the near infrared region of the spectrum.

The NIR oven emits radiation over a wide range including visible and midinfrared peaking between 800 and 1200 nm. The NIR oven used here has a fixed emitter module with reflectors and a platform moving at a line speed which determines the NIR exposure time. The FTO glass substrate (2.2 mm thick glass with a 600 nm layer of FTO deposited commercially by APCVD) and an uncoated glass substrate of identical thickness were exposed to 12.5 s of NIR radiation and measured upon exit with an IR camera to estimate the surface temperature. Using predetermined emissivity values (0.92 for uncoated glass and 0.16 for FTO coated glass), the temperature upon exit of the NIR unit was estimated for both substrates at varying intensities of NIR output, seen in Figure 2.

The substrates were held at room temperature prior to each 12.5 s NIR exposure and reached their maximum temperature immediately prior to exit from under the emitter module. Both substrates heat upon exposure to the NIR photons which interact with the substrate rapidly releasing thermal energy. The FTO coated glass reaches a higher temperature than the uncoated glass of the same thickness across all NIR intensities due to the enhanced absorption of the FTO layer in the NIR region (due to a larger concentration of free carriers). The increased temperature induced by the presence of the 600 nm FTO layer is significant with an increase of over 300°C observed for 100% intensity NIR exposure.

3.2. Heating of TiO_2 Paste. The conventional method for creating the mesoporous TiO_2 necessary for a DSC is to heat the deposited film (typically containing a binder and solvent) to 450°C for 30 min removing the binder to form a mesoporous structure and promoting particle interconnectivity.

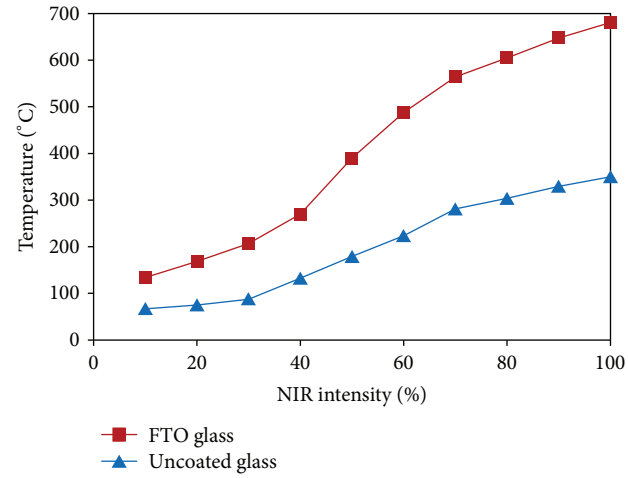

Figure 2: Temperature of FTO glass and uncoated glass after 12.5 s of NIR exposure at varying NIR intensities.

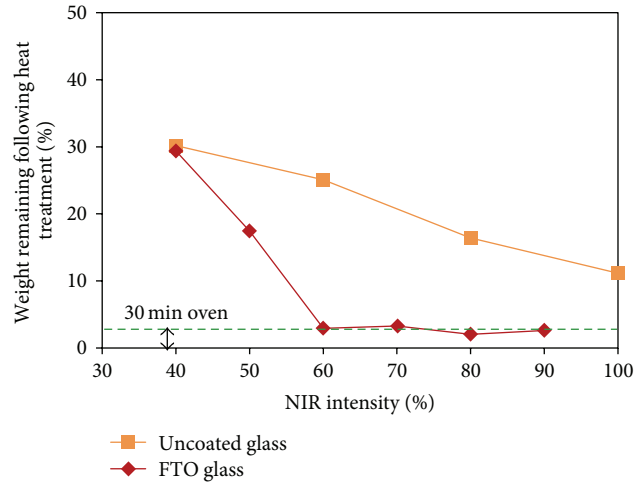

Figure 3: Weight of material remaining in the TiO_2 paste as measured by thermogravimetric analysis of 12.5 s NIR exposed TiO_2 paste on FTO glass and uncoated glass. The weight loss observed for a 30-minute oven treatment is shown as a dotted line (- - -).

Figure 2 shows that this temperature is reached at 60% NIR intensity for FTO coated glass but is not reached for uncoated glass. This would suggest that full binder removal and sintering on FTO coated glass should only occur for NIR lamp powers in excess of 60%. TiO_2 paste was deposited onto the glass substrates via doctor blading then exposed to NIR for 12.5 s. The dry film thickness was 9 μm on both FTO coated glass and uncoated glass. In order to assess the effectiveness of binder removal, any remaining binder was identified through a subsequent offline thermogravimetric analysis where samples of the remaining material were heated from 30 to 600°C and the weight loss was recorded. Figure 3 shows the weight of material remaining in each NIR heated film versus the intensity of the NIR lamps for both FTO coated and uncoated glass substrates.

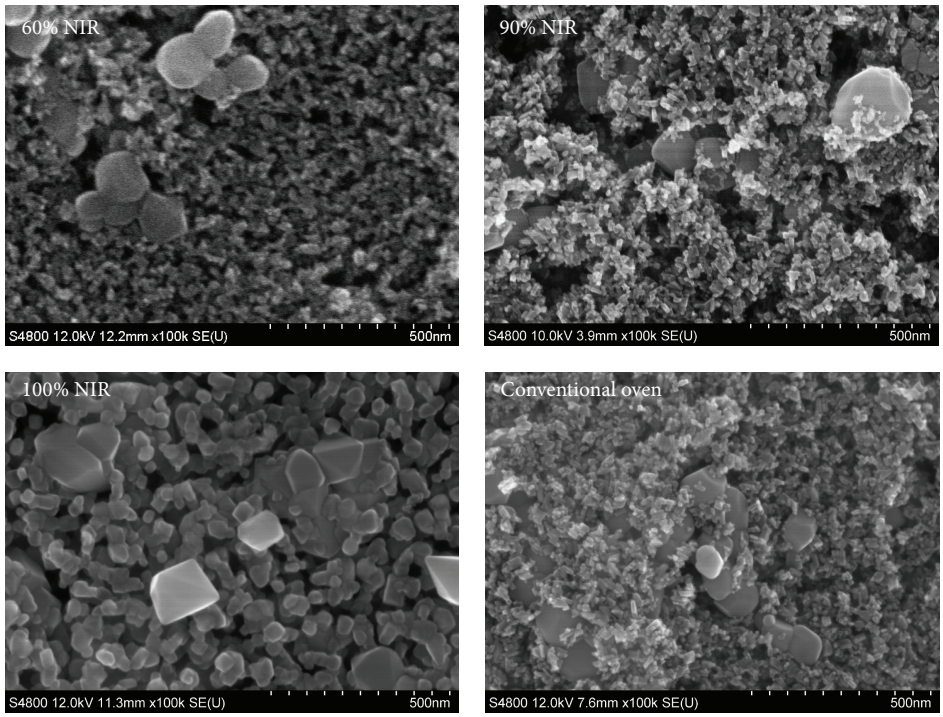

Figure 4: SEM micrographs of TiO_2 films on FTO glass heated with 12.5 s of NIR radiation at 60%, 90%, and 100% as well as a conventionally sintered film.

The weight remaining following each NIR treatment illustrates and confirms the stark difference in temperature reached between FTO glass and uncoated glass, reinforcing the integral role the FTO has in increasing absorption and enabling this technique to work for glass at higher temperatures. Following 40% NIR intensity treatment, a similar weight of material remains for both the FTO glass and uncoated glass because the threshold for binder combustion has not been achieved for either substrate. At 40%, sufficient temperature has been reached on both substrates in order to remove the solvents (this typically constitutes approximately 60% of the overall weight).

At 60% NIR intensity, the FTO glass exceeds the required temperature to combust the binder leaving 3.8% of material remaining. There is insufficient thermal energy to remove all binder resulting in 3.8% of decomposed binder remaining. The subsequent TGA weight loss of the TiO_2 film is equivalent to that of conventionally sintered (30 min, 450°C) films. No further significant weight loss is seen at higher NIR power settings indicating that binder removal is complete at powers of 70% and above. It is observed that all samples, even where binder removal is considered complete, experience some subsequent weight loss during the TGA experiment. This can be attributed to water adsorption by the TiO_2 when left in ambient laboratory conditions.

The uncoated glass reaches a maximum temperature of 350°C at 100% power. It might be expected that some binder combustion could take place at this temperature but the total thermal energy received in this short 12.5 sec timeframe is insufficient for complete combustion; so, binder still remains in the film.

The FTO layer absorbs NIR photons via free carrier absorption causing a sudden release of thermal energy effectively turning the FTO layer into a hot plate. This creates an extreme temperature gradient between the FTO and the TiO_2 paste which allows thermal conduction to act upon the paste extremely quickly, directionally driving out the solvent and binder. The combustion of the TiO_2 paste binder is essential for the formation of efficient working electrodes for DSCs. In addition, the TiO_2 nanoparticles require sintering to provide intimate contact in order to fabricate a mesoporous film for efficient charge transport. In order to assess particle interconnectivity, SEM images were taken of 12.5 s NIR heated TiO_2 films on FTO glass (Figure 4).

The commercial paste contains 20 nm sized anatase particles and 150 nm scattering particles. At 90% NIR intensity, the TiO_2 film is comparable to the conventional oven film. At 60% NIR intensity, the film appears less porous due to some charred binder remaining. At 100% NIR intensity, there appear to be some growth of the anatase crystals and the possible appearance of larger tetragonal rutile. This was previously observed for the NIR heating of TiO_2 paste on titanium metal substrates and was attributed to a high peak metal temperature of 785°C [16]. The maximum temperature for FTO glass at this intensity is predicted to be around 680°C but its lower thermal conductivity compared to titanium could mean it was subjected to a sufficient temperature for grain growth over a longer period.

3.3. NIR Heated TiO_2 Films in Dye-Sensitized Solar Cells. 12.5 s NIR heated TiO_2 films were constructed into working electrodes for DSCs and compared to conventionally heated

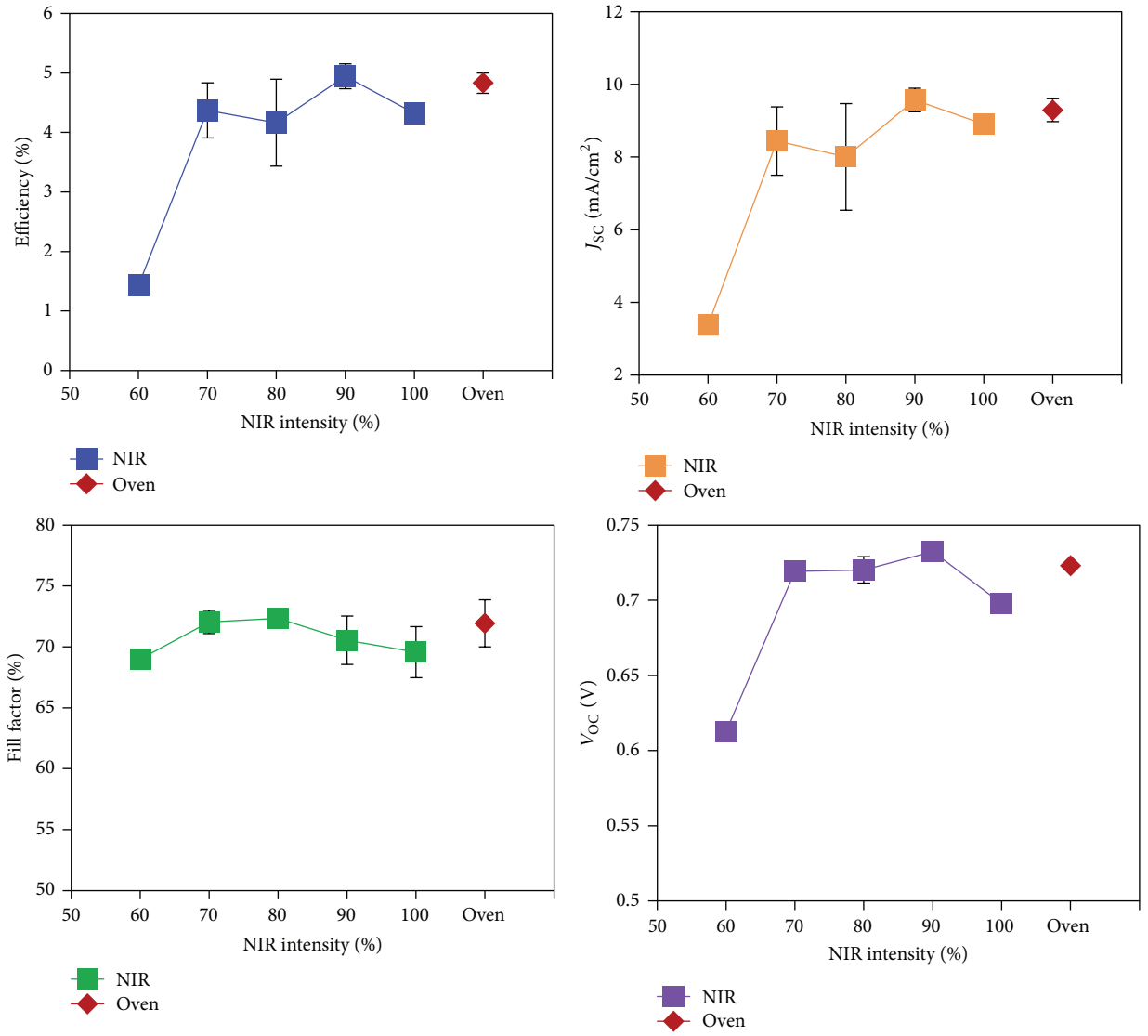

Figure 5: Mean IV parameters for DSC devices with NIR and conventionally sintered working electrodes, error bar representing standard deviation of 3 devices.

working electrodes; a summary of the IV data is shown in Figure 5.

A maximum efficiency of 5.2% was obtained for a 90% NIR DSC compared to 5.0% for a conventionally heated DSC for these simply constructed 1 cm^2 area devices. The current density is the dominant influence on the efficiency for these cells due to the differing degrees of sintering for the TiO_2 particles; the fill factors and open circuit voltages are fairly consistent for all cells except 60% NIR which has a poor V_{OC}. At 60% NIR intensity, although the majority of the binder was removed, the particles do not appear to be sufficiently sintered for charge transport as indicated by the low current density. With a maximum temperature of 487°C after 12.5 s exposure, it is unlikely that the film would have been at a sufficiently high enough temperature for long enough to allow complete sintering during the time scale. At 70% NIR, the maximum temperature is about 80°C higher allowing enough heat energy to transfer to the particles to sinter more effectively. This continues to 648°C at 90% NIR intensity where sintering comparable to conventional sintering has occurred. At 100% NIR, the efficiency is slightly lower due to a lower surface area for dye adsorption as suggested by the SEM in Figure 4 because the high temperature has accelerated the sintering into crystal growth. Optoelectronic transient measurements as described in [20] were carried out in order to determine the charge transport and recombination kinetics in fast sintered devices. Figure 6 summarises the data obtained from these measurements.

Figure 6(a) shows the charge density at V_{OC} measured via charge extraction. All devices except those exposed to 60% NIR lamp intensity have near identical charge densities, which could indicate a similar density of electronic trap states. The 60% NIR heated samples have received insufficient thermal energy in order to sinter effectively resulting in a

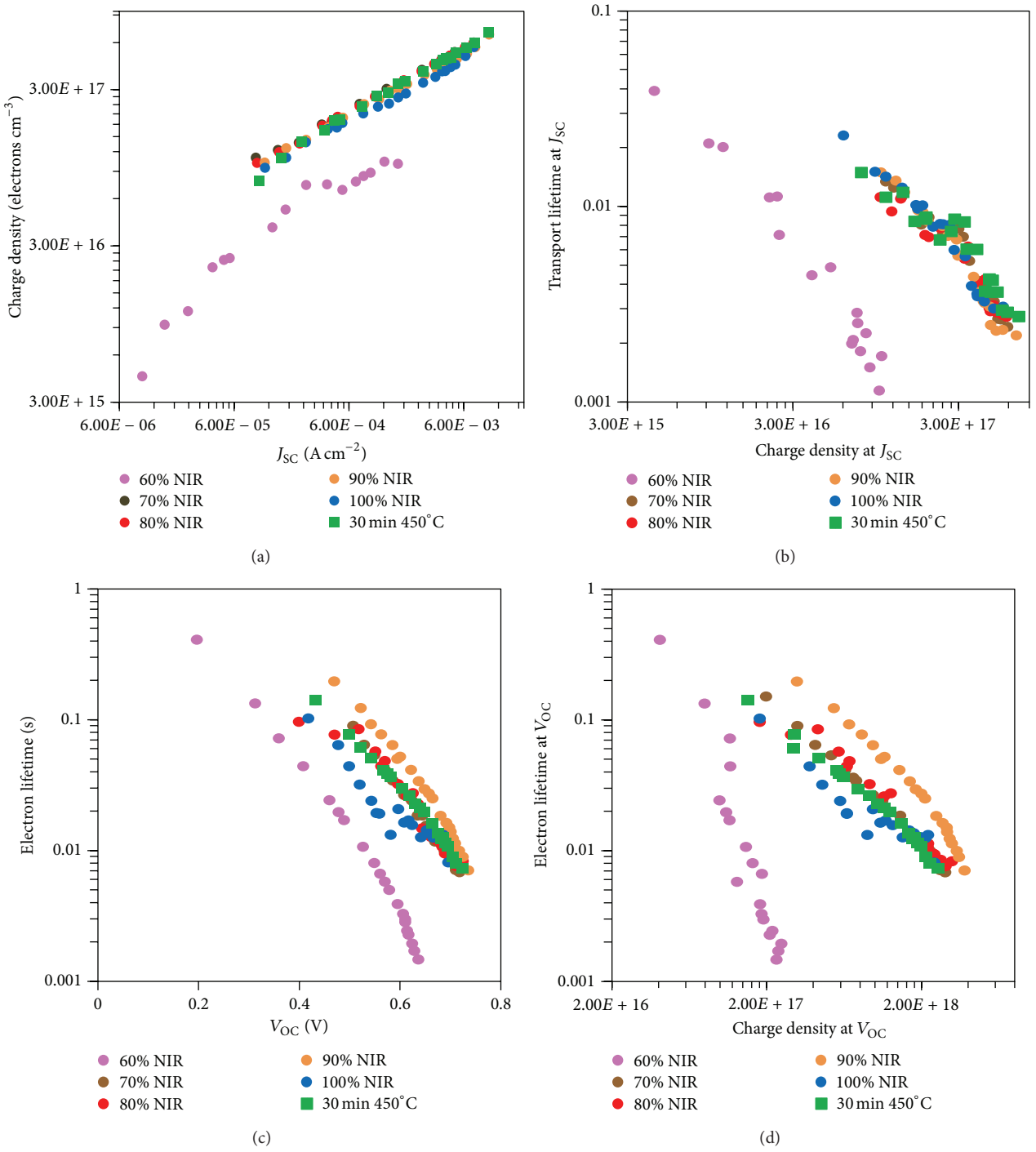

FIGURE 6: Optoelectronic transient measurements for (a) charge density versus J_{SC} m, (b) transport lifetime versus charge density at J_{SC}, (c) electron lifetime versus V_{OC}, and (d) electron lifetime at V_{OC} versus charge density at V_{OC}.

decrease in trap states at the particle interface boundaries. Figure 6(b) shows the short circuit current transient lifetime versus charge density at J_{SC} giving an indication of electron transport kinetics as a function of charge density. The faster transport kinetics seen in the 60% NIR heated devices could also be attributed to fewer trap states. For all other devices, the transport lifetime is similar, suggesting that particle connectivity and trap density are equivalent in all the NIR heated devices exposed to 70% lamp power and above and in the conventionally sintered devices. Figure 6(c) shows electron lifetime at open circuit voltage versus V_{OC}, and Figure 6(d) shows the electron lifetime at open circuit voltage versus the

charge density at open circuit voltage, both giving an indication of recombination kinetics. The fastest rate of recombination is observed in the 60% NIR heated devices and may be attributed to insufficient binder removal. A broad trend is then observed whereby electron lifetime increases with increasing NIR intensity. This supports an increasing density of trap states [20] as a consequence of improved sintering from increased thermal energy during NIR exposure. The exception to this trend is that devices sintered using the highest NIR lamp intensity at 100% show an increase in the rate of recombination. The explanation for this is uncertain but the increased crystal size shown in SEM and the slight decrease in J_{SC} seen in these devices could indicate a decrease in dye loading whilst still allowing recombination to take place so that there is more available surface area for recombination with I_3^- than in the other devices where dye loading is greater.

4. Conclusions

FTO glass heats significantly and rapidly upon exposure to NIR radiation due to FTO's high concentration of free carriers that facilitate enhanced absorption in the NIR/IR region over glass alone. The sudden rise in temperature effectively turns the FTO layer into a hot plate and creates an extreme temperature gradient between the FTO and the TiO_2 paste which allows thermal conduction to act upon the paste extremely quickly, directionally driving out the solvent and the binder. At sufficient lamp intensity, this enables both complete solvent and binder removal of TiO_2 paste and the creation of a mesoporous 9 μm interconnected TiO_2 layer in 12.5 s.

When assembled into DSCs, these films performed identically to conventionally sintered films with a heating time 144 times faster. The ability of NIR radiation to sinter TiO_2 films in 12.5 s has been demonstrated on metallic substrates but this is the first time it has been shown on glass based substrates. The rapid heating of FTO glass could be applied to other similar solution processable electronic devices such as fuel cells or other solar cells.

Conflict of Interests

The authors declare that there is no conflict of interests regarding the publication of this paper.

Acknowledgments

The authors would like to thank the EPSRC and TSB for supporting this work through the SPECIFIC Innovation and Knowledge Centre. The authors would also like to gratefully acknowledge the Welsh Government for their support through the Sêr Solar Programme. The authors gratefully acknowledge the help and support of Dr. Brian O'Regan for his advice and support in building the transient instrumentation.

References

[1] B. O'Regan and M. Gratzel, "A low-cost, high-efficiency solar cell based on dye-sensitized colloidal TiO_2 films," *Nature*, vol. 353, no. 6346, pp. 737–740, 1991.

[2] A. Yella, H.-W. Lee, H. N. Tsao et al., "Porphyrin-sensitized solar cells with cobalt (II/III)-based redox electrolyte exceed 12 percent efficiency," *Science*, vol. 334, no. 6056, pp. 629–634, 2011.

[3] T. Watson, C. Charbonneau, M. Carnie, I. Mabbett, M. Cherrington, and D. Worsley, "Addressing bottlenecks in dye-sensitized solar cell manufacture using rapid near-infrared heat treatments," *MRS Proceedings*, vol. 1447, mrss12-1447-v06-04, 2012.

[4] H. Lindström, A. Holmberg, E. Magnusson, L. Malmqvist, and A. Hagfeldt, "A new method to make dye-sensitized nanocrystalline solar cells at room temperature," *Journal of Photochemistry and Photobiology A: Chemistry*, vol. 145, no. 1-2, pp. 107–112, 2001.

[5] H. Lindström, E. Magnusson, A. Holmberg, S. Södergren, S.-E. Lindquist, and A. Hagfeldt, "A new method for manufacturing nanostructured electrodes on glass substrates," *Solar Energy Materials and Solar Cells*, vol. 73, no. 1, pp. 91–101, 2002.

[6] H. Lindström, A. Holmberg, E. Magnusson, S.-E. Lindquist, L. Malmqvist, and A. Hagfeldt, "A new method for manufacturing nanostructured electrodes on plastic substrates," *Nano Letters*, vol. 1, no. 2, pp. 97–100, 2001.

[7] S. Uchida, M. Tomiha, N. Masaki, A. Miyazawa, and H. Takizawa, "Preparation of TiO_2 nanocrystalline electrode for dye-sensitized solar cells by 28 GHz microwave irradiation," *Solar Energy Materials and Solar Cells*, vol. 81, no. 1, pp. 135–139, 2004.

[8] G. Mincuzzi, L. Vesce, M. Liberatore, A. Reale, A. Di Carlo, and T. M. Brown, "Laser-sintered TiO_2 films for dye solar cell fabrication: an electrical, morphological, and electron lifetime investigation," *IEEE Transactions on Electron Devices*, vol. 58, no. 9, pp. 3179–3188, 2011.

[9] H. Kim, R. Auyeung, M. Ollinger, G. Kushto, Z. Kafafi, and A. Piqué, "Laser-sintered mesoporous TiO_2 electrodes for dye-sensitized solar cells," *Applied Physics A*, vol. 83, no. 1, pp. 73–76, 2005.

[10] H. Pan, D. Lee, S. H. Ko, C. P. Grigoropoulos, H. K. Park, and T. Hoult, "Fiber laser annealing of indium-tin-oxide nanoparticles for large area transparent conductive layers and optical film characterization," *Applied Physics A: Materials Science and Processing*, vol. 104, no. 1, pp. 29–38, 2011.

[11] H. Pan, S. H. Ko, N. Misra, and C. P. Grigoropoulos, "Laser annealed composite titanium dioxide electrodes for dye-sensitized solar cells on glass and plastics," *Applied Physics Letters*, vol. 94, no. 7, Article ID 071117, 2009.

[12] G. Mincuzzi, L. Vesce, A. Reale, A. di Carlo, and T. M. Brown, "Efficient sintering of nanocrystalline titanium dioxide films for dye solar cells via raster scanning laser," *Applied Physics Letters*, vol. 95, no. 10, Article ID 103312, 2009.

[13] G. Mincuzzi, M. Schulz-Ruhtenberg, L. Vesce et al., "Laser processing of TiO_2 films for dye solar cells: a thermal, sintering, throughput and embodied energy investigation," *Progress in Photovoltaics: Research and Applications*, vol. 22, no. 3, pp. 308–317, 2014.

[14] H. Y. Jin, J. Y. Kim, J. A. Lee et al., "Rapid sintering of TiO_2 photoelectrodes using intense pulsed white light for flexible dye-sensitized solar cells," *Applied Physics Letters*, vol. 104, no. 14, Article ID 143902, 2014.

[15] T. Watson, I. Mabbett, H. Wang, L. Peter, and D. Worsley, "Ultrafast near infrared sintering of TiO_2 layers on metal substrates for dye-sensitized solar cells," *Progress in Photovoltaics: Research and Applications*, vol. 19, no. 4, pp. 482–486, 2011.

[16] M. J. Carnie, C. Charbonneau, P. R. F. Barnes et al., "Ultra-fast sintered TiO_2 films in dye-sensitized solar cells: phase variation, electron transport and recombination," *Journal of Materials Chemistry A*, vol. 1, no. 6, pp. 2225–2230, 2013.

[17] M. Cherrington, T. C. Claypole, D. Deganello, I. Mabbett, T. Watson, and D. Worsley, "Ultrafast near-infrared sintering of a slot-die coated nano-silver conducting ink," *Journal of Materials Chemistry*, vol. 21, no. 21, pp. 7562–7564, 2011.

[18] C. Charbonneau, K. Hooper, M. Carnie et al., "Rapid radiative platinisation for dye-sensitised solar cell counter electrodes," *Progress in Photovoltaics: Research and Applications*, 2013.

[19] S. Ito, N.-L. C. Ha, G. Rothenberger et al., "High-efficiency (7.2%) flexible dye-sensitized solar cells with Ti-metal substrate for nanocrystalline-TiO_2 photoanode," *Chemical Communications*, no. 38, pp. 4004–4006, 2006.

[20] P. R. F. Barnes, K. Miettunen, X. Li et al., "Interpretation of optoelectronic transient and charge extraction measurements in dye-sensitized solar cells," *Advanced Materials*, vol. 25, no. 13, pp. 1881–1922, 2013.

[21] R. G. Gordon, "Criteria for choosing transparent conductors," *MRS Bulletin*, vol. 25, no. 8, pp. 52–57, 2000.